Observation of the Adler-Bell-Jackiw chiral anomaly in a Weyl semimetal

Chenglong Zhang, Su-Yang Xu, Ilya Belopolski, Zhujun Yuan, Ziquan Lin, Bingbing Tong, Nasser Alidoust, Chi-Cheng Lee, Shin-Ming Huang, Hsin Lin, Madhab Neupane, Daniel S. Sanchez, Hao Zheng, Guang Bian, Junfeng Wang, Chi Zhang, Titus Neupert, M. Zahid Hasan, and Shuang Jia.

arXiv:1503.02630

Observation of the Adler-Bell-Jackiw chiral anomaly in a Weyl semimetal

Chenglong Zhang et al. arXiv:1503.02630

Here, for the first time, we report experimental studies of the first Weyl semimetal TaAs which reveals the chiral anomaly in its magnetotransport.

Unlike most metals that become more insulating or resistive under an external magnetic field,

we observe that our high mobility TaAs samples, quite remarkably, become more conductive as a magnetic field is applied along the direction of the current for certain ranges of the field and

its magnetoconductance disperses quadratically which is nearly independent of temperatures below 20 K, but depends strongly on the relative angles between the electric and magnetic fields.

1. Observation of the chiral magnetic effect in $ZrTe_5$,
Qiang Li, Dmitri E. Kharzeev, et al., arxiv:1412.6543

Here we report on the first observation of chiral magnetic effect (CME) through the measurement of magneto-transport in zirconium pentatelluride, $ZrTe_5$.

2. Observation of the chiral anomaly induced negative magneto-resistance in 3D Weyl semi-metal TaAs,
Xiaochun Huang et al., arxiv:1503.01304

In the present paper, we report the first experimental evidence for the long-anticipated negative magneto-resistance generated by the chiral anomaly in a newly predicted time-reversal invariant Weyl semi-metal material TaAs.

Outline:

1. What are semimetals?

2. Theoretical background of the chiral anomaly in condensed matter physics.

3. Recent experiments on quadratic negative magnetoresistance in semimetals.

4. Main conclusions.

The conduction and valence bands touch at discrete points, with a linear dispersion relation in all three momentum space directions moving away from the Weyl node.

$$\mathcal{H} = \pm v_F \boldsymbol{\sigma} \cdot \mathbf{k}$$

Weyl point or node is a point of contact between two nondegenerate bands in the first Brillouin zone.

the sign in front refers to two possible chiralities of the band contact point

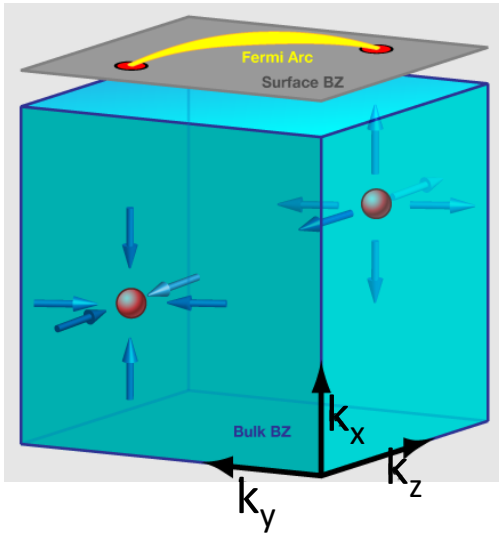

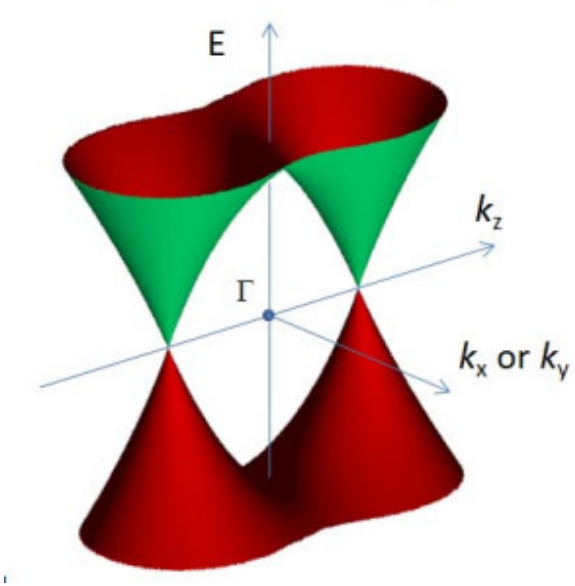

Review:
Hosur, Qi arxiv:1309.4464,
Burkov 1502.07609

Weyl SM In the presence of the magnetic field B.

Landau levels:

$$\epsilon_n = v_F \mathrm{sign}(n)\sqrt{2\hbar|n|eB + (\hbar \boldsymbol{k}\cdot\hat{\boldsymbol{B}})^2},\ n = \pm 1, \pm 2, \ldots$$

$$\epsilon_0 = -\chi \hbar v_F \boldsymbol{k}\cdot\hat{\boldsymbol{B}}$$

Pairs of Weyl nodes with $\chi=\pm 1$.

The zero LL disperses only one way for each Weyl node:

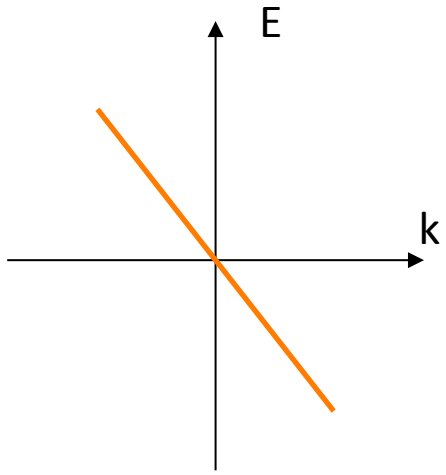

Left-handed Weyl

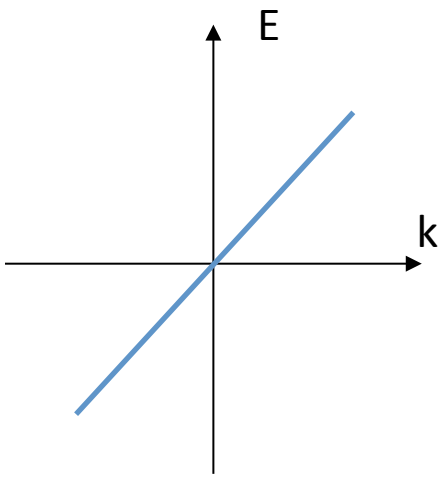

Right-handed Weyl

Derivation of the positive magnetoconductance:

Qiang Li, Dmitri E. Kharzeev, et al., arxiv:1412.6543

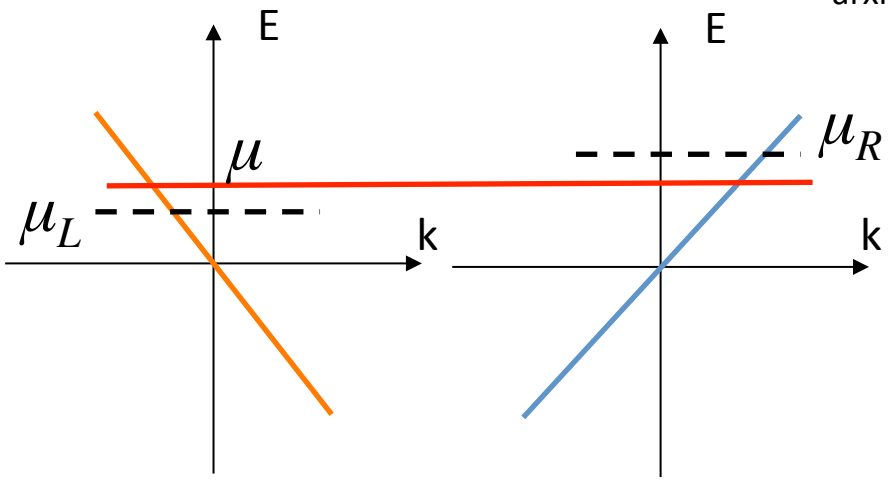

If the energy degeneracy between the L and R handed fermions is broken:

$$\mu_5 \equiv (\mu_R - \mu_L)/2$$

The density of the chiral charge:

$$\rho_5 \equiv (\rho_R - \rho_L)/2$$

Parallel external electric and magnetic fields generate the chiral charge with a rate that is proportional to the product of electric and magnetic fields.
Adler; Bell and Jackiw (1969):

$$\frac{d\rho_5}{dt} = \frac{e^2}{4\pi^2\hbar^2 c}\vec{E}\cdot\vec{B}$$

Chiral anomaly = nonconservation of the numbers of
Weyl fermions of distinct chiralities.

The left- and right-handed fermions can mix through chirality-changing scattering,

$$\frac{d\rho_5}{dt} = \frac{e^2}{4\pi^2\hbar^2 c}\vec{E}\cdot\vec{B} - \frac{\rho_5}{\tau_V}$$

τ_V is the chirality changing scattering.

$$\rho_5 = \frac{e^2}{4\pi^2\hbar^2 c}\vec{E}\cdot\vec{B}\;\tau_V \qquad t \gg \tau_V$$

$$\rho_5 = \frac{\mu_5^3}{3\pi^2 v^3} + \frac{\mu_5}{3v^3}\left(T^2 + \frac{\mu^2}{\pi^2}\right)$$

$$\mu_5 = \frac{3}{4}\frac{v^3}{\pi^2}\frac{e^2}{\hbar^2 c}\frac{\vec{E}\cdot\vec{B}}{T^2 + \frac{\mu^2}{\pi^2}}\tau_V \qquad \mu_5 \ll \mu, T$$

If the densities of L and R handed fermions are different the system develops a net electric current. Chiral Magnetic Effect:

$$\vec{J}_{\mathrm{CME}} = \frac{e^2}{2\pi^2}\;\mu_5\;\vec{B}$$

Fukushima et al. PRD, 78 (2008)

$$J^i_{\rm CME} = \frac{e^2}{\pi\hbar}\,\frac{3}{8}\frac{e^2}{\hbar c}\,\frac{v^3}{\pi^3}\,\frac{\tau_V}{T^2+\frac{\mu^2}{\pi^2}}\,B^iB^kE^k \equiv \sigma^{ik}_{\rm CME}\,E^k$$

When E and B are parallel, the CME conductivity is:

$$\sigma^{zz}_{\rm CME} = \frac{e^2}{\pi\hbar}\,\frac{3}{8}\frac{e^2}{\hbar c}\,\frac{v^3}{\pi^3}\,\frac{\tau_V}{T^2+\frac{\mu^2}{\pi^2}}\,B^2$$

The CME-related positive magnetoconductivity will dominate the classical negative magnetoconductivity, provided that:

$$\frac{\tau_V}{\tau_{tr}}\frac{1}{\mu\tau_{tr}} > 1$$

Son, Spivak PRB (2013),
Burkov PRL (2014)

It is possible to derive the coupled diffusion equations
for the total and chiral charge densities in the presence of the magnetic field:

$$\frac{\partial n}{\partial t} = D\frac{\partial^2 n}{\partial z^2} + \Gamma\frac{\partial n_a}{\partial z},$$
$$\frac{\partial n_a}{\partial t} = D\frac{\partial^2 n_a}{\partial z^2} - \frac{n_a}{\tau_a} + \Gamma\frac{\partial n}{\partial z}$$

$$\Gamma = eB/2\pi^2 g(\epsilon_F)$$

$$n_a = \Gamma\tau_a\frac{\partial n}{\partial z}$$

$$\sigma = \sigma_0 + \frac{e^4 B^2 \tau_a}{4\pi^4 g(\epsilon_F)}$$

Son, Spivak PRB (2013),
Burkov PRL (2014)

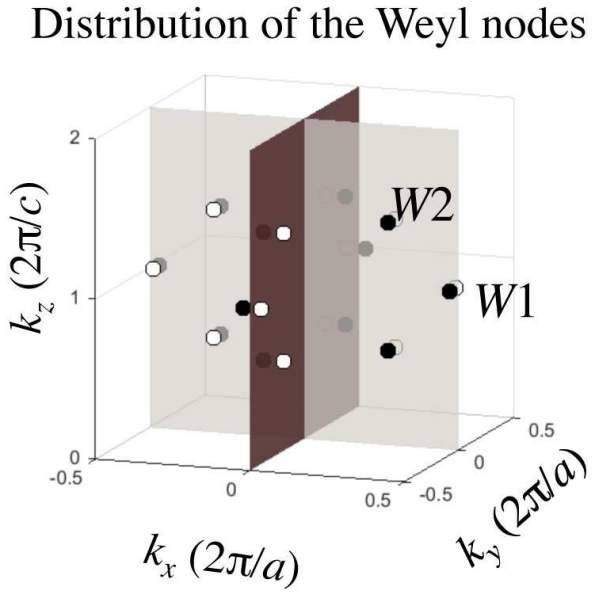

How about experiment?

arXiv:1503.02630 and 1503.01304

TaAs

Distribution of the Weyl nodes throughout the first bulk Brillouin zone, where a total of 24 Weyl nodes are present and the sign of their chiral charges are color coded in black and white. 1501.00755, 1501.00060

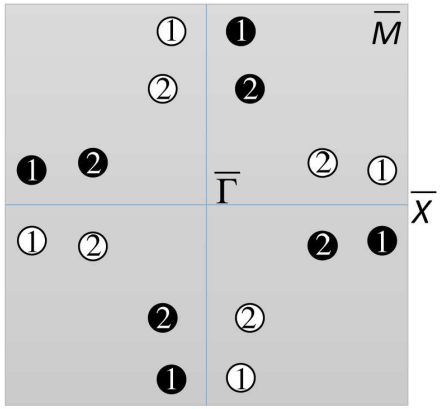

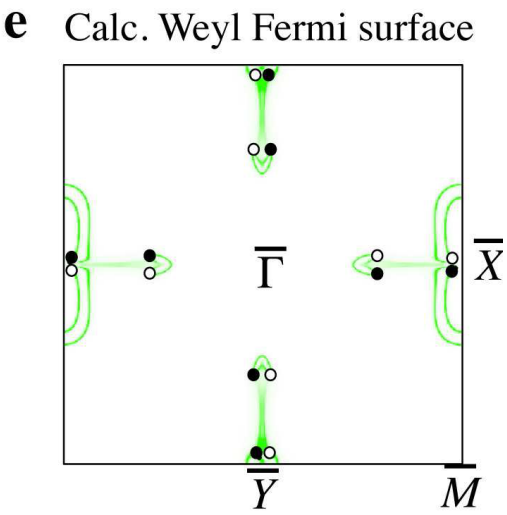

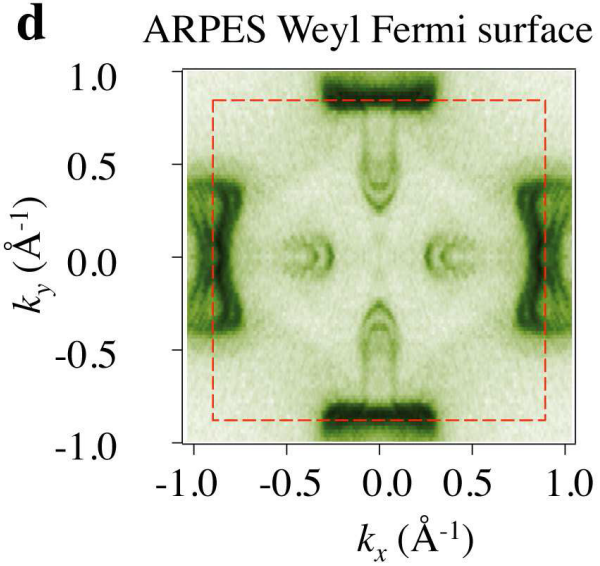

ARPES Fermi surface map of the (001) cleaving plane of TaAs, clearly resolving Fermi arcs near the X point, Y point, midpoint of the X point and Gamma point, and midpoint of the Y point and Gamma point of the surface Brillouin zone.

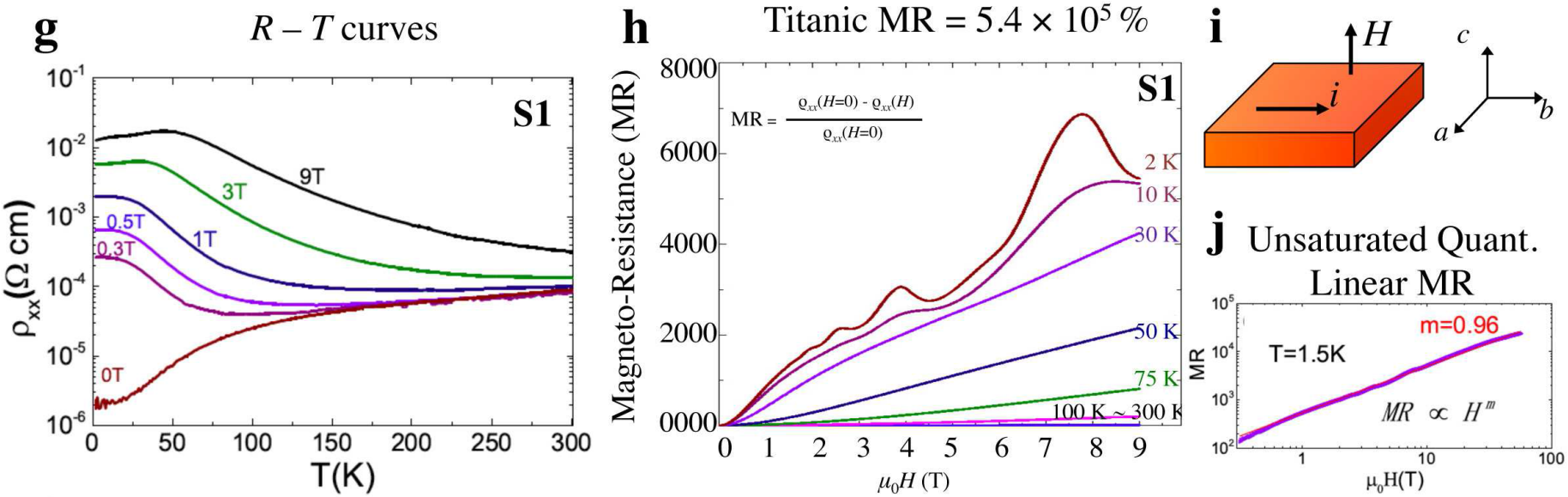

Temperature dependence of resistivity at different magnetic fields perpendicular to the current.

Magneto-resistance at various temperatures.

a Quantum oscillations

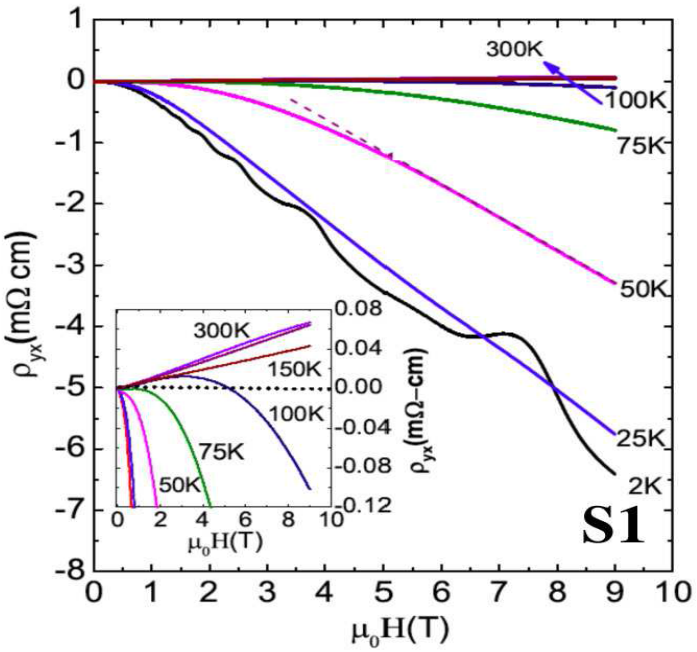

Hall resistivity versus magnetic field
in the temperature range from 2 to 300 K.

f

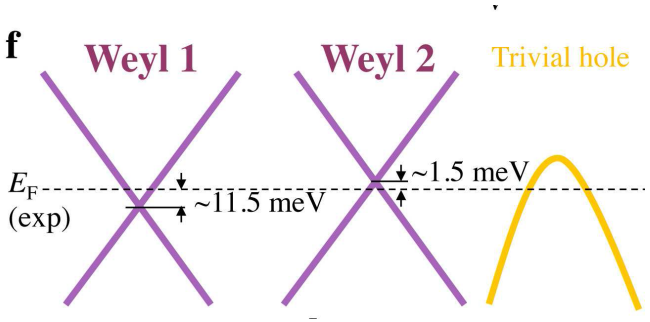

$$\frac{\tau_V}{T^2 + \frac{\mu^2}{\pi^2}} B^2$$

The magnetoconductivity was measured in a configuration where the applied electric and magnetic fields are parallel.

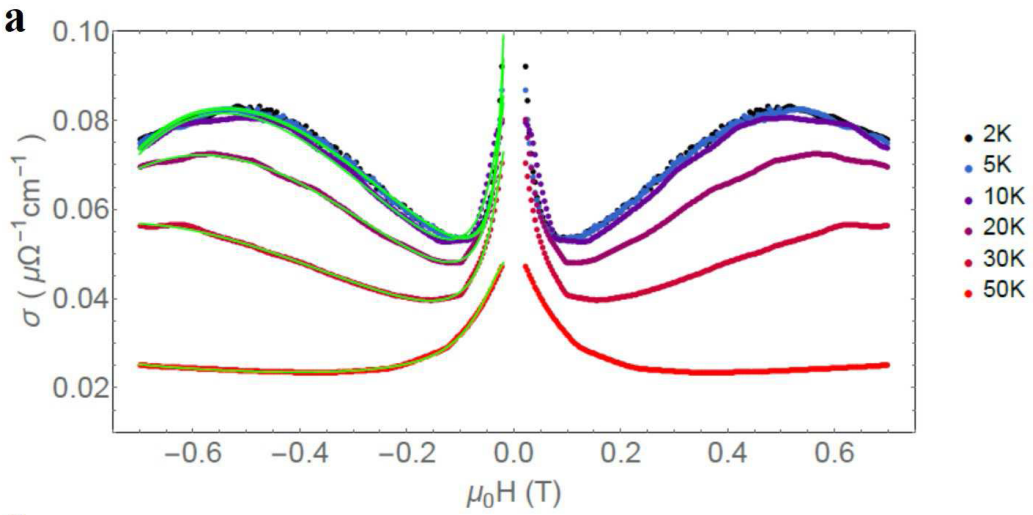

Magnetoconductivity at different temperatures and fits to the data.

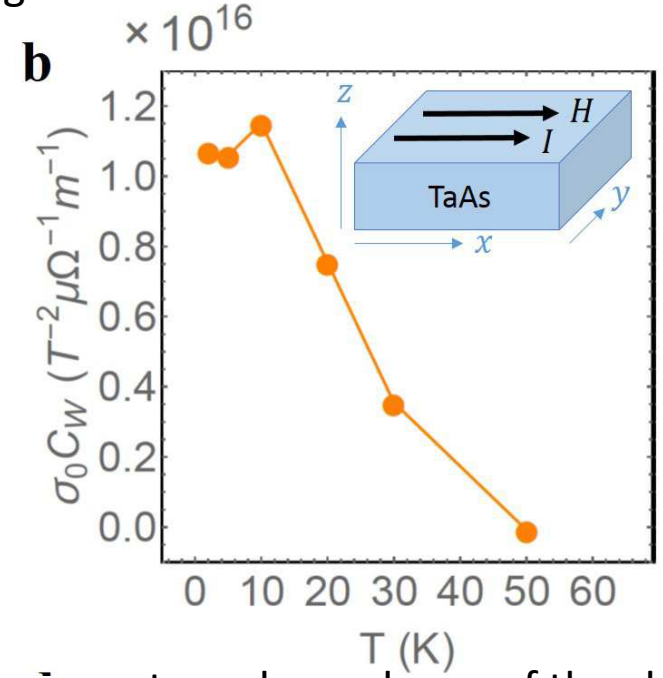

Temperature-dependence of the chiral anomaly contribution to the magnetoconductivity as obtained from the fits in panel.

$$\frac{\tau_V}{T^2 + \frac{\mu^2}{\pi^2}} B^2$$

$$\sigma(H) = \left(\sigma_0 + a\sqrt{H}\right)\left(1 + C_W H^2\right) + \frac{1}{\rho + A\,H^2} + \frac{1}{\rho' + A'\,H^2},$$

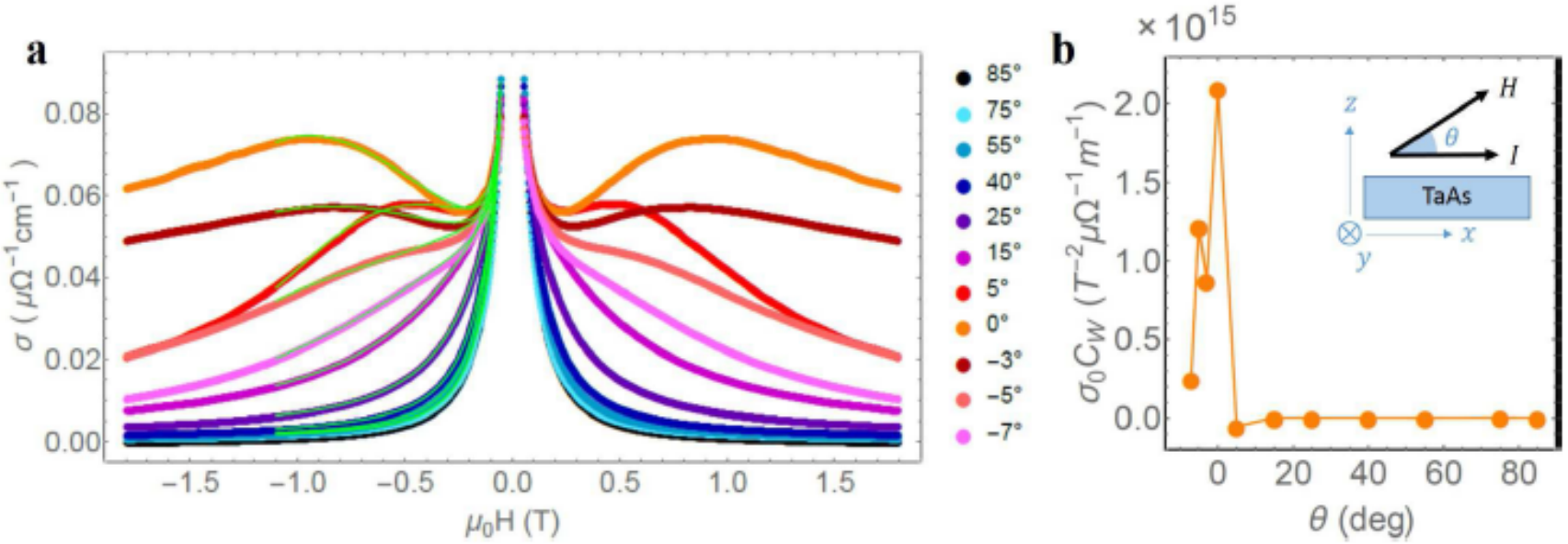

Magnetoconductivity at different angles and T = 2 K as well as fits to the data

Angle-dependence of the chiral anomaly contribution to the magnetoconductivity as obtained from the fits.

Two different samples. The chiral anomaly contribution to the conductivity for two different Fermi energies. Anomalous contribution scaled as $(1/E_F)^2$

Main conclusions:

1. The consequence of CME in transport is a quadratic negative magnetoresistance, which dominates all other contributions to magnetoresistance under certain conditions.

2. The CME is argued to be observed through measurement of magnetotransport in $ZrTe_5$ and TaAs. These materials electronic band structure is consistent with the semimetal.

3. One of the promising directions is the interplay between the chiral anomaly and superconductivity.

Recent review: Burkov, 1502.07609